Eur. Phys. J. E (2015) **38**: 106
DOI 10.1140/epje/i2015-15106-4

The European Physical Journal E

Regular Article

Wave-particle interaction in the Faraday waves*

N. Francois[a], H. Xia, H. Punzmann, and M. Shats[b]

Research School of Physics and Engineering, The Australian National University, Canberra, ACT 2601, Australia

Received 18 August 2015
Published online: 2 October 2015 – © EDP Sciences / Società Italiana di Fisica / Springer-Verlag 2015

Abstract. Wave motion in disordered Faraday waves is analysed in terms of oscillons or quasi-particles. The motion of these oscillons is measured using particle tracking tools and it is compared with the motion of fluid particles on the water surface. Both the real floating particles and the oscillons, representing the collective fluid motion, show Brownian-type dispersion exhibiting ballistic and diffusive mean squared displacement at short and long times, respectively. While the floating particles motion has been previously explained in the context of two-dimensional turbulence driven by Faraday waves, no theoretical description exists for the random walk type motion of oscillons. It is found that the r.m.s velocity $\langle \tilde{u}_{\mathrm{osc}} \rangle_{\mathrm{rms}}$ of oscillons is directly related to the turbulent r.m.s. velocity $\langle \tilde{u} \rangle_{\mathrm{rms}}$ of the fluid particles in a broad range of vertical accelerations. The measured $\langle \tilde{u}_{\mathrm{osc}} \rangle_{\mathrm{rms}}$ accurately explains the broadening of the frequency spectra of the surface elevation observed in disordered Faraday waves. These results suggest that 2D turbulence is the driving force behind both the randomization of the oscillons motion and the resulting broadening of the wave frequency spectra. The coupling between wave motion and hydrodynamic turbulence demonstrated here offers new perspectives for predicting complex fluid transport from the knowledge of wave field spectra and vice versa.

Introduction

Faraday waves [1] are parametrically excited perturbations that appear on a liquid surface when the latter is vertically vibrated. Those waves can generate a variety of two-dimensional patterns [2–5]. Though such patterns can be described via the nonlinear interactions of waves [6], an alternative approach has emerged after the discovery of the localised oscillating excitations, termed oscillons [7]. Oscillons have been discovered in a variety of flows. The first parametrically driven stationary oscillons were discovered on the water surface in a resonator [8]. Later oscillons were found in granular layers [7], in thin layers of highly dissipative fluids [9], in non-Newtonian fluids [10], in strongly dissipative liquids vibrated at two frequencies [11] and in a very narrow vertically vibrated cell [12]. The oscillonic nature of Faraday waves on the water surface was also revealed and discussed in the context of the order-to-disorder transition in strongly nonlinear three-dimensional Faraday ripples [13]. It was proposed that the shape of oscillons in physical space determines the shape of the frequency spectra of the nonlinear Faraday waves. Later, the horizontal mobility of oscillons was studied to understand mechanisms leading to the generation of extreme wave events [14].

In parallel with the better understanding of the quasi-particle nature of the Faraday surface ripples, a remarkable progress has been made in studying the motion of the fluid particles of which these waves are comprised [15–17]. It was found that at low dissipation and sufficiently high vertical acceleration, the motion of fluid particles on the water surface reproduces in detail the motion of fluid in two-dimensional turbulence [18]. In particular, the Kolmogorov-Kraichnan spectrum $E_k \propto k^{-5/3}$ of flow kinetic energy characterizes the fluid motion in the horizontal plane. The existence of the inverse energy cascade was confirmed by measurements of the Kolmogorov flux relation from the third-order velocity structure function. The inverse cascade transfers spectral energy from small to large scales in 2D turbulence and leads in bounded flow to the accumulation or condensation of spectral energy at the boundary size scale. The effect of spectral condensation was observed in the Faraday wave-driven 2D turbulence [16]. Several works on the Lagrangian statistics of floating tracers revealed that fluid transport follows the classical Taylor single-particle dispersion [19,20]. In particular, it was found that the fluid particle dispersion is determined by a single measurable Lagrangian scale L_L comparable to the forcing scale L_f. This scale L_L determines the diffusion coefficient in 2D turbulence via $D = \langle \tilde{u} \rangle_{\mathrm{rms}} L_L$, where $\langle \tilde{u} \rangle_{\mathrm{rms}}$ is the root-mean-squared velocity in isotropic turbulence.

* Contribution to the Topical Issue "Multi-scale phenomena in complex flows and flowing matter" edited by Luca Biferale, Massimo Cencini, Alessandra Lanotte and Mauro Sbragaglia.

[a] e-mail: Nicolas.Francois@anu.edu.au
[b] e-mail: Michael.Shats@anu.edu.au

In this paper we ask the following question: is it possible to bridge the gap between the quasi-particle description of the Faraday waves and the statistical characteristics of the fluid motion on the surface? Recent experimental advances allow us to compare simultaneously the motion of the wave phase with that of fluid particles from both Lagrangian and Eulerian viewpoints. Here we study Lagrangian and Eulerian statistics of the oscillon motion and compare them with those of the fluid motion to show that it is possible to predict transport on the surface of water perturbed by the Faraday waves from the knowledge of the wave fields and vice versa. In particular, these results demonstrate that the broadening of the wave spectra can be predicted if the 2D turbulence energy is known.

Experimental results

To visualise the surface elevation in Faraday waves, we employ a version of the profilometry technique, the diffusive light imaging (see, *e.g.*, [17]). The technique allows tracking the positions of oscillons in the x-y plane with good spatial and temporal resolution. Moreover, in this study, we simultaneously track the horizontal motion of the oscillons and of the fluid particles by seeding the fluid surface with floating tracers (particle diameter $\approx 200\,\mu$m). This allows the motion of these two entities to be compared from two different description viewpoints:

a) The Lagrangian viewpoint, which is the trajectory-based representation of a motion. Using particle tracking technique to describe Faraday waves has only been introduced recently [14]. In this respect, the Lagrangian motion of oscillons can be understood as the horizontal motion of the local wave phase.
b) The Eulerian viewpoint, which characterises the motion as the temporal evolution of a spatial field.

Faraday waves are formed in a circular container (178 mm diameter, 30 mm deep) filled with a liquid whose depth is larger than the wavelength of the perturbations at the surface (deep water approximation). The container is vertically vibrated by an electrodynamic shaker. The forcing is monochromatic and set to $f_0 = 60\,$Hz. The amplitude a of the vertical acceleration imposed by the shaker is measured by an accelerometer. An electronic controller uses the real-time feedback of the accelerometer to control the shaker acceleration and forcing frequency. The acceleration threshold for the parametric excitation of Faraday waves is $a_c \approx 0.6g$ at $f_0 = 60\,$Hz.

Figure 1(a) shows a snapshot of the wave field as observed by using the diffusive light imaging techniques. The temporal evolution of a $8 \times 8\,\mathrm{cm}^2$ wave field is captured by a fast camera at 120 frames per second. The intensity of the transmitted light is inversely proportional to the wave heights: darker blobs correspond to the wave crests in fig. 1(a). White dots within the dark blobs mark the local oscillon maximum. The motion of these maxima is analysed by performing particle tracking velocimetry. Figure 1(b) shows the mean-squared displacement $\langle \delta r^2 \rangle_{\rm osc} = \langle |\vec{r}(t)_{\rm osc} - \vec{r}(0)_{\rm osc}|^2 \rangle$ of an oscillon moving along the trajectory $\vec{r}(t)_{\rm osc}$ from its initial position $\vec{r}(0)$. The mean-squared horizontal displacement (MSD) shows ballistic behaviour at short times and has a diffusive behaviour at longer times

$$\langle \delta r^2 \rangle_{\rm osc} \approx \langle \tilde{u}^2_{\rm osc} \rangle t^2, \quad \text{at} \quad t \ll T_{L_{\rm osc}}, \tag{1}$$
$$\langle \delta r^2 \rangle_{\rm osc} \approx 2\langle \tilde{u}^2_{\rm osc} \rangle T_{L_{\rm osc}} t, \quad \text{at} \quad t \gg T_{L_{\rm osc}}. \tag{2}$$

Here $u_{\rm osc}$ is the oscillon velocity, $T_{L_{\rm osc}} = \int_0^\infty \rho(t)\mathrm{d}t$ is the Lagrangian integral time, which can be obtained from the Lagrangian velocity autocorrelation function

$$\rho(t) = \langle \mathbf{u}_{\rm osc}(t_0 + t)\mathbf{u}_{\rm osc}(t_0) \rangle / \langle \tilde{u}^2_{\rm osc} \rangle, \tag{3}$$

where $\langle \tilde{u}^2_{\rm osc} \rangle$ is the velocity variance. The oscillon velocity autocorrelation function is a decaying integrable function of time, as seen in fig. 1(c). It characterises the memory loss process of the random motion of oscillons in the horizontal plane. In fig. 1(c), the estimated Lagrangian integral time for the oscillons motion is of the order of 0.15 s, consistent with the change in the scaling of $\langle \delta r^2 \rangle_{\rm osc}$ in fig. 1(b). Figure 1(d) shows the root-mean squared oscillon velocity $\langle \tilde{u}_{\rm osc} \rangle_{\rm rms}$ as a function of the vertical acceleration a. The velocity increases linearly with a.

These results have an interesting consequence on the interpretation of the frequency spectrum of the Faraday waves which is commonly measured as an Eulerian quantity, *i.e.* the wave elevation is measured locally in space. The random walk of oscillons about the observation point in the x-y plane should lead to the broadening of the frequency spectra by random Doppler shift. This thermal broadening should then be given by $\Delta f_{\rm th} = \langle \tilde{u}_{\rm osc} \rangle_{\rm rms}/\lambda$, where λ is the characteristic scale of the oscillon for a given excitation frequency. It has been previously shown that this scale is related to the wavelength derived from the linear dispersion relation of capillary waves [13]. Figure 1(e) shows the wave number spectra of the surface elevation in these experiments at two levels of acceleration. The characteristic size of the oscillons here remains constant and is $\lambda = 2\pi/k_{\max} \approx 7.4\,$mm. Figure 1(f) shows the expected broadening $\Delta f_{\rm th}$ of the frequency spectra versus vertical acceleration.

We compare the spectral broadening expected from the "thermal" motion of oscillons with spectral measurements of the surface elevation at fixed point in space. The Eulerian frequency spectra measured at five levels of vertical acceleration are shown in fig. 2. As the vertical acceleration is increased, the spectra broaden exhibiting pronounced exponential tails: $E_w \propto \exp(-Bf)$. The parameter $1/B$ characterises the spectral broadening of the first subharmonic of f_0. As seen in the inset of fig. 2(b), $1/B$ scales linearly with the vertical acceleration a and it is close to the expected broadening of the frequency spectra in fig. 1(f).

It is interesting to compare the motion of the actual fluid particles on the water surface with the motion of the oscillons, or the wave phase. We have previously reported that both motions seem qualitatively distinct [16], however these differences have never been quantified. Figure 3(a) shows the MSD of fluid particles and oscillons. It

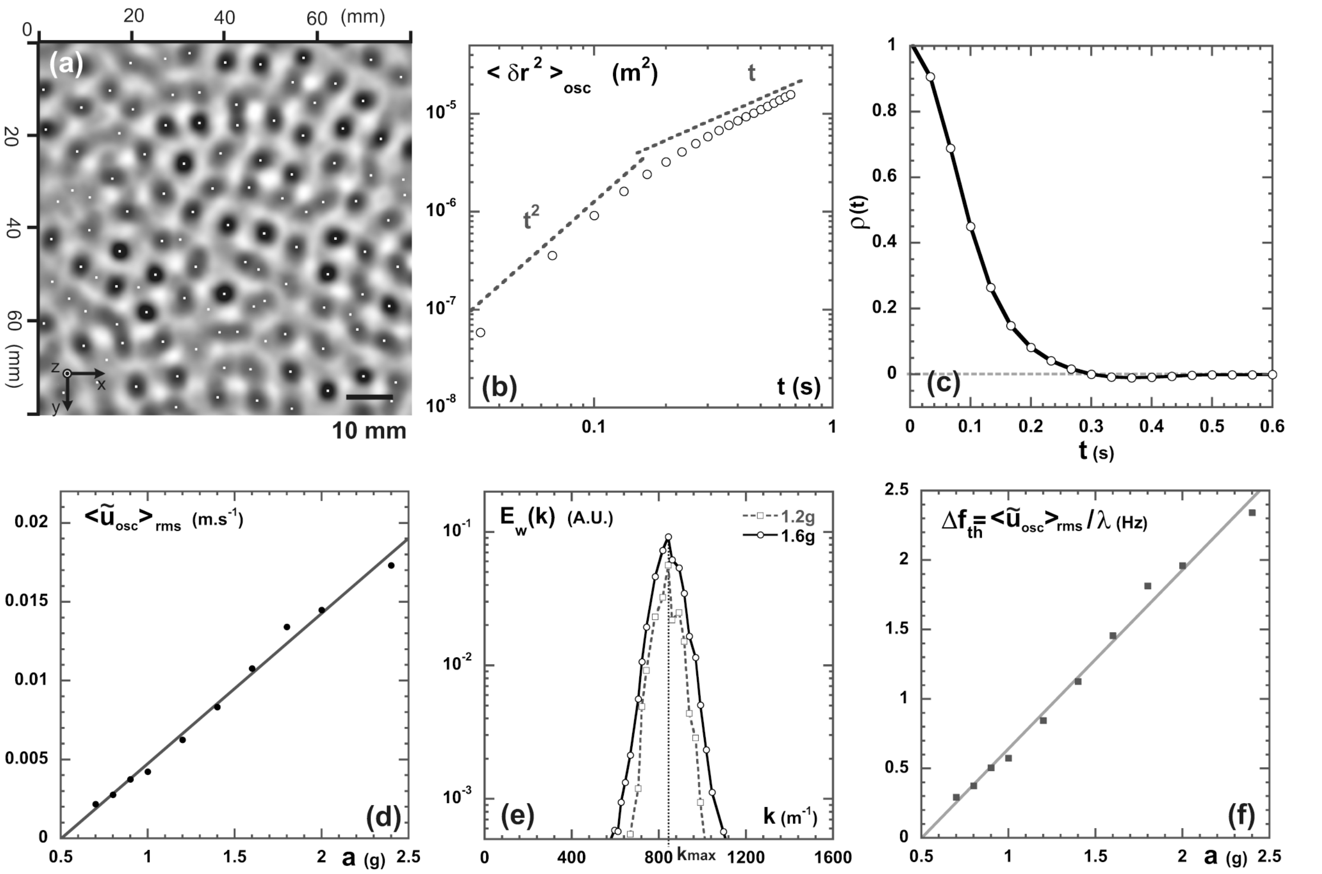

Fig. 1. (a) An image of the Faraday waves using the diffusive light imaging technique. Peaks and troughs appear as dark and white blobs. Local wave maxima are detected (white dots within dark blobs) and their motion is tracked using PTV techniques. (b) The mean-squared horizontal displacement of oscillons $\langle \delta r^2 \rangle_{\mathrm{osc}}$ away from their initial position as a function of time. (c) The Lagrangian velocity autocorrelation function $\rho(t)$ of the oscillons motion. Data shown in (b) and (c) were measured at the vertical acceleration of $a = 1.6g$ using over 2000 oscillon trajectories. (d) RMS value of the oscillon velocity fluctuations $\langle \tilde{u}_{\mathrm{osc}} \rangle_{\mathrm{rms}}$ in the x-y plane *versus* the vertical acceleration a. (e) Wave number power spectra of the surface elevation at different vertical acceleration ($a = 1.2g$ and $a = 1.6g$). (f) Predicted Doppler shift $\Delta f_{\mathrm{th}} = \langle \tilde{u}_{\mathrm{osc}} \rangle_{\mathrm{rms}}/\lambda$ of the oscillon frequency spectra *versus* the vertical acceleration a.

shows that both entities share similar Lagrangian properties, such as a diffusive transport regime at long times [19]. The theory of single fluid particle dispersion driven by turbulent agitation dates back to Taylor [21]. To our knowledge, there is no theory that predicts the diffusive motion of oscillons at the water surface. The main difference between both motions stems from the Lagrangian integral scale which characterizes the diffusive motion and corresponds to the step length of the associated Brownian walk. The Lagrangian integral scale is computed as the product of the r.m.s velocity by the Lagrangian integral time. In the following, the integral scales of the fluid motion and of the oscillon motion are named L_L and $L_{L\mathrm{osc}}$, respectively. L_L is constant and roughly equal to 3.3 mm in fully developed turbulence ($a > 1g$ for $f_0 = 60\,\mathrm{Hz}$) while $L_{L\mathrm{osc}}$ increases with a and is markedly smaller than L_L as shown in fig. 3(b).

For the same broad range of vertical accelerations, we also compare the r.m.s. fluid particle velocity $\langle \tilde{u} \rangle_{\mathrm{rms}}$ with the r.m.s oscillon velocity $\langle \tilde{u}_{\mathrm{osc}} \rangle_{\mathrm{rms}}$. Figure 4 shows the ratio $\langle \tilde{u} \rangle_{\mathrm{rms}}/\langle \tilde{u}_{\mathrm{osc}} \rangle_{\mathrm{rms}}$ as a function of a. At low accelerations this ratio increases with a, however when 2D turbulence develops manifested by the Kolmogorov $k^{-5/3}$ Eulerian spectrum (see the inset in fig. 4), the ratio remains constant at the level $\langle \tilde{u} \rangle_{\mathrm{rms}}/\langle \tilde{u}_{\mathrm{osc}} \rangle_{\mathrm{rms}} \approx 3$ in the broad range of accelerations.

Discussion and conclusions

Broadening of spectral harmonics of disordered capillary waves has been discussed with respect to the Faraday waves, *e.g.* [22,23], but never in the context of the horizontal turbulent fluid motion.

The results presented here point to a strong connection between the random-walk-type motion of fluid particles on the surface and that of the oscillons, or the local wave phases. First, both exhibit ballistic dispersion at times less than Lagrangian velocity correlation time. Second, both show fast decaying velocity autocorrelation functions. Third, the observed r.m.s. horizontal velocities

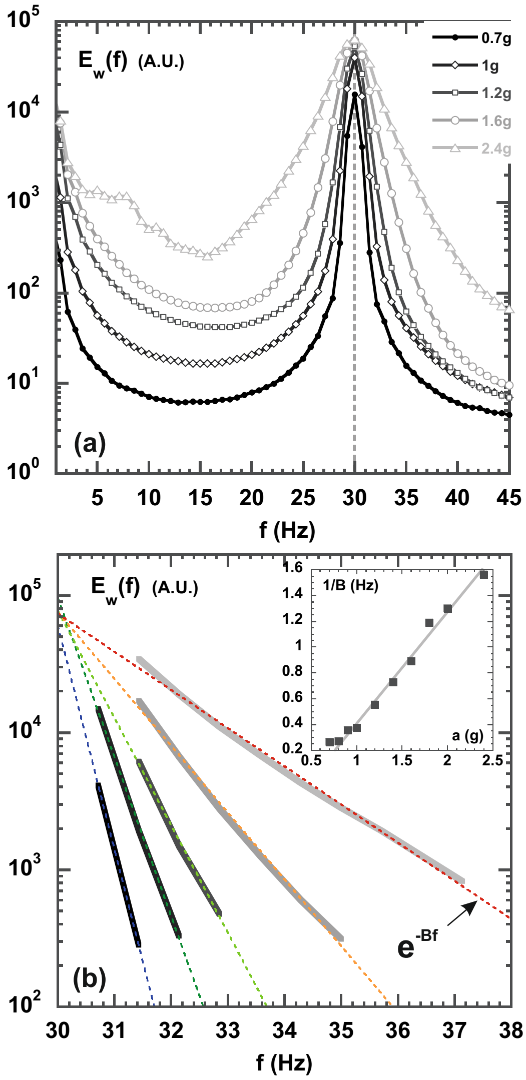

Fig. 2. (a) Eulerian frequency power spectra of the Faraday waves elevation at different vertical acceleration a. (b) Close up on the broadening of the subharmonic. The dashed lines correspond to the exponential fit $\exp(-Bf)$. Inset: spectral width $1/B$ of the subharmonic *versus* a.

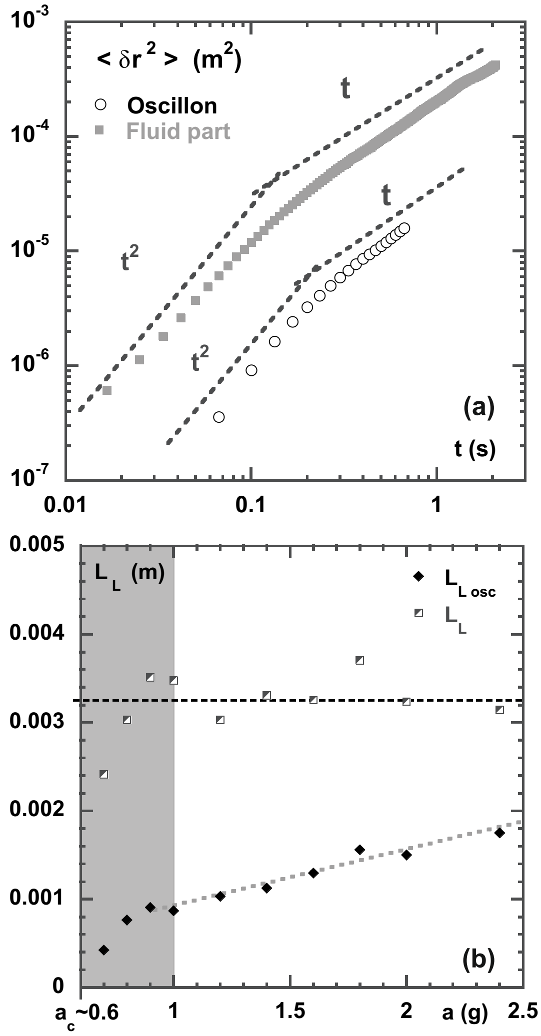

Fig. 3. (a) MSD of the fluid particles and of the oscillons at the same acceleration $a = 1.6g$. (b) Lagrangian integral length scale of the horizontal motion of fluid particles L_L and of oscillons L_{Losc} *versus* the vertical acceleration a.

of oscillons are very well correlated with the r.m.s. velocities of the Faraday-wave-driven turbulence.

Qualitatively, the fact that the ratio of the fluid particle velocities is approximately three times higher than that of oscillons (fig. 4) can be understood as follows. The Eulerian correlation length of the fluid particles velocity in fully developed turbulence is shorter than the oscillon size [19]. The motion of an oscillon is a collective fluid motion of many independent particles. For the data discussed here the Eulerian correlation length for the particle velocity is $L_E = 2.2\,\mathrm{mm}$, while the oscillon size, as discussed above, is $\lambda \approx 7.4\,\mathrm{mm}$, roughly a factor of 3 larger.

The random motion of oscillons leads to the observation of exponential tails in the broadened frequency spectra of fig. 2(b). The origin of these tails was discussed in ref. [13]. The surface elevation by a single oscillon is well described by $h(x) \sim \mathrm{sech}(ax)$. The horizontal motion of an oscillon in its random walk is slow, $T_L = 0.15\,\mathrm{s}$ in fig. 1(c) compared with the period of the vertical oscillations of 0.033 s (30 Hz in this experiment). Such random motion of vertically oscillating quasi-particles leads to a shape of the frequency spectrum in figs. 2(a-b) given by $E(f) \sim \mathrm{sech}^2[B(f - f_h)]$, where $f_h = 30\,\mathrm{Hz}$ is the first subharmonic frequency. The spectral broadening measured as $1/B$ is consistent with the Doppler shift computed from the measured r.m.s. velocity of the oscillons. The latter is directly related to the presence of 2D turbulence on the water surface.

Summarising, we present the analysis of the Faraday wave motion in disordered wave fields in water and compare it with the measurements of the turbulent motion of the surface fluid particles. This study suggests that 2D turbulence is the driving force behind both the randomisation of the oscillon motion and the resulting broadening of the wave frequency spectra.

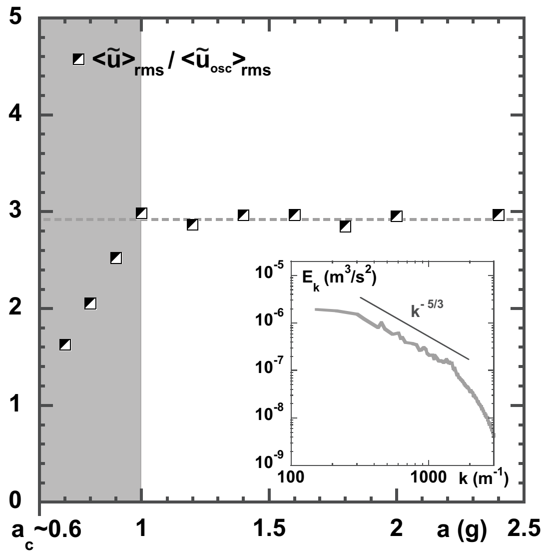

Fig. 4. Ratio of the RMS value of the fluid particle velocity fluctuations over the oscillon velocity fluctuations at different acceleration a. Inset: Eulerian wave number spectrum of the horizontal kinetic energy of the fluid particles at $a = 1.6g$.

Both, particles and quasi-particles, exhibit Taylor dispersion. The mean-squared displacement is ballistic ($\propto t^2$) at short times and diffusive ($\propto t$) at times longer than the corresponding Lagrangian velocity correlation time T_L. Perhaps the most remarkable observation is that in fully developed turbulence, at the vertical acceleration $a \geq 1g$ (see fig. 4), the ratio of the r.m.s. velocities of the surface fluid particles and of the wave phases remains constant at the level of $\langle\tilde{u}\rangle_{\rm rms}/\langle\tilde{u}_{\rm osc}\rangle_{\rm rms} \approx 3$. This result needs to be further investigated theoretically. If proven universal, this offers a method of determining the diffusion coefficient in the Faraday-wave-driven 2D turbulence using the information only about the wave phase motion since $D = \langle\tilde{u}\rangle_{\rm rms}L_L$. Here $L_L = \langle\tilde{u}\rangle_{\rm rms}T_L \approx 0.7L_f$ is the Lagrangian correlation length related to the forcing scale L_f [19,20] and $\langle\tilde{u}\rangle_{\rm rms} \approx 3\langle\tilde{u}\rangle_{\rm osc}$.

This work was supported by the Australian Research Council's Discovery Projects funding scheme (DP150103468). HX would like to acknowledge the support by the Australian Research Council's Future Fellowship (FT140100067).

References

1. M. Faraday, Philos. Trans. R. Soc. London **121**, 319 (1831).
2. A. Kudrolli, J.P. Gollub, Physica D **97**, 133 (1996).
3. D.I. Goldman, M.D. Shattuck, Sung Joon Moon, J.B. Swift, H.L. Swinney, Phys. Rev. Lett. **90**, 104302 (2003).
4. A.V. Kityk, J. Embs, V.V. Mekhonoshin, C. Wagner, Phys. Rev. E **72**, 036209 (2005).
5. I. Shani, G. Cohen, J. Fineberg, Phys. Rev. Lett. **104**, 184507 (2010).
6. M.C. Cross, P.C. Hohenberg, Rev. Mod. Phys. **65**, 851 (1993).
7. P.B. Umbanhowar, F. Melo, H.L. Swinney, Nature **382**, 793 (1986).
8. J. Wu, R. Keolian, I. Rudnick, Phys. Rev. Lett. **52**, 1421 (1984).
9. O. Lioubashevski, H. Arbell, J. Fineberg, Phys. Rev. Lett. **76**, 3959 (1996).
10. O. Lioubashevski, Y. Hamiel, A. Agnon, Z. Reches, J. Fineberg, Phys. Rev. Lett. **83**, 3190 (1999).
11. H. Arbell, J. Fineberg, Phys. Rev. Lett. **81**, 4384 (1998).
12. J. Rajchenbach, A. Leroux, D. Clamond, Phys. Rev. Lett. **107**, 024502 (2011).
13. M. Shats, H. Xia, H. Punzmann, Phys. Rev. Lett. **108**, 034502 (2012).
14. H. Xia, T. Maimbourg, H. Punzmann, M. Shats, Phys. Rev. Lett. **109**, 114502 (2012).
15. A. von Kameke, F. Huhn, G. Fernández-García, A.P. Muñuzuri, V. Pérez-Muñuzuri, Phys. Rev. Lett. **107**, 074502 (2011).
16. N. Francois, H. Xia, H. Punzmann, M. Shats, Phys. Rev. Lett. **110**, 194501 (2013).
17. N. Francois, H. Xia, H. Punzmann, M. Shats, Phys. Rev. X **4**, 021021 (2014).
18. R. Kraichnan, Phys. Fluids **10**, 1417 (1967).
19. H. Xia, N. Francois, H. Punzmann, M. Shats, Nat. Commun. **4**, 2013 (2013) doi: 10.1038/ncomms3013.
20. H. Xia, N. Francois, H. Punzmann, M. Shats, Phys. Rev. Lett. **112**, 104501 (2014).
21. G.I. Taylor, Proc. London Math. Soc. **20**, 196 (1921).
22. D. Snouck, M.-T. Westra, W. van de Water, Phys. Fluids **21**, 025102 (2009).
23. H. Punzmann, M. Shats, H. Xia, Phys. Rev. Lett. **103**, 064502 (2009).